

Effect of Hydraulic Properties of Fill and Geocomposite Drainage Materials on Seepage Response in Reinforced Earth Walls

Avirut Chinkulkijniwat¹, Suksun Horpibulsuk², Duc Bui Van³, Somjai Yubonchit⁴,
Thanakorn Rakkob³

1-Associate Professor, Center of Excellence in Civil Engineering, School of Civil Engineering, Suranaree University of Technology, 111 University Avenue, Muang District, Nakhon Ratchasima 30000 Thailand

2- Professor and Director, Center of Excellence in Innovation for Sustainable Infrastructure Development, Chair of School of Civil Engineering, Suranaree University of Technology, 111 University Avenue, Muang District, Nakhon Ratchasima 30000 Thailand

3-Ph. D scholar, School of Civil Engineering, Suranaree University of Technology, 111 University Avenue, Muang District, Nakhon Ratchasima 30000 Thailand

4-Research fellowship, School of Civil Engineering, Suranaree University of Technology, 111 University Avenue, Muang District, Nakhon Ratchasima 30000 Thailand

Email: avirut@sut.ac.th

Abstract

This research aims to investigate the effect of water retention characteristic of the fill soil and drainage material (geocomposite) on seepage responses in mechanical stabilized earth walls using geocomposite as an alternative drainage system. A set of experiments on physical models was conducted such that the dataset obtained from the tests were used to calibrate the numerical models. Obtained calibrated numerical models were then used to perform a series of parametric calculation. The studied parameters were van Genuchten parameters (g_a and g_n) and coefficient of permeability (k) of the relevant materials. Results from the parametric study indicate that the water retention characteristic of the soil outside the reinforced zone plays little role to the hydraulic response of the soil inside the reinforced zone. However, the coefficient of permeability of the soil outside the reinforced zone plays important role to the level of the phreatic surface inside the reinforced zone. Hence, the coefficient of permeability of the soil outside the reinforced zone must be taken into account as designing drainage system.

Keywords: Mechanical Stabilized Earth Wall, Geocomposite, Drainage System, Numerical Modeling.

1. INTRODUCTION

Instability of mechanical stabilised earth (MSE) walls in mountainous areas, where seasonally heavy rainfall is encountered, is often attributed to ineffective drainage systems (Koerner and Soong 2001, Shibuya et al. 2007). Shibuya et al. (2007) reported an investigated results from a catastrophic failure of a reinforced earth wall occurred in Yabu, Japan, in 2004, after a typhoon. Although the design codes were used to design and build the reinforced earth wall, in which the drainage was positioned at the bottom of the wall from drainage pipes but the area behind the wall was not fully covered; hence, there was an insufficient capacity in the drainage system installed. It was concluded that conventional drainage systems were not applicable in mountainous areas where there was a large amount and/or high level of groundwater.

The material conventionally used as the drainage medium for MSE walls is well-graded gravel. This is becoming increasingly expensive, and effective installation of this material as a vertical drainage layer is difficult in the field (Koerner and Soong 2001; Shibuya et al. 2007). An alternative to the use of well-graded gravel is to provide drainage through the use of geocomposites (Koerner and Soong 2000; Koerner 2005; Chen et al. 2007) which comprise a core material with a large flow channel (e.g., geonet) covered by two nonwoven geotextile layers. Geocomposites provide a hydraulic conductivity approximately 10 to 100 times higher than that of compacted backfills. Geocomposites offer numerous advantages over the conventional method of drainages such as ease of transportation and installation; the use of geocomposites does not add significantly to the weight of the soil in the backfill due to its light weight; construction time is significantly reduced as geocomposites is used, hence economic benefit. McKean and Inouye (2001) reported a successful field case study using geocomposites to prevent water flowing behind a retaining wall. This MSE wall was reported successfully performed for period of around of 14 years.

Although there have been many reported case studies on the successful implementation of geocomposites as alternative drainage systems, there is no known work that incorporates the water retention characteristic (WRC)

of geotextiles in these reported numerical simulations. Previous studies indicate that geotextiles' water retention characteristics are similar to those of coarse-grained soils such as gravels and sands (Stormont et al. 1997; Lafleur et al. 2000; Morris 2000; Stormont and Morris 2000; Knight and Kotha 2001; Iryo and Rowe 2003, 2004; Bouazza et al. 2006; Bathurst et al. 2007, 2009; Nahlawi et al. 2007). Therefore, an insight into the influences of WRC of geotextiles on flow response is necessary to allow for a more effective and appropriate use of geocomposites in MSE walls.

This research was conducted using a large-scale flow test through an MSE wall in which an L-shape geocomposite drain was installed. A set of needed instrumentations were positioned in the physical models to assess the flow and deformation responses during the tests, they were four standpipe piezometers, 10-time domain reflectometer (TDR) probes and 10 surface settlement plates. Numerical analyses were subsequently conducted using the Plaxis-2D finite element modelling software to investigate the effect of the hydraulic properties on the water flow taking place in the MSE wall. The numerical computation of flow results was mainly presented in terms of phreatic surface and effective saturation profiles.

2. THEORETICAL BACKGROUND

The governing equation for transient water flow in a two dimensional homogeneous anisotropic material within an unsaturated porous medium is as follows

$$k_x \frac{\partial^2 h}{\partial x^2} + k_y \frac{\partial^2 h}{\partial y^2} = \frac{\partial \theta}{\partial t}$$

where θ is the volumetric water content, h is the total head, k_x and k_y are the unsaturated coefficients of permeability in the x - and y -directions, and t is time. To solve Equation 1, constitutive equations related to θ , k_x and k_y to h are required. Iryo and Rowe (2003, 2004) concluded that there is considerable evidence to suggest that van Geuchten (VG) (van Genuchten, 1980) and van Genuchten-Mualem (VGM) models, which combine the van Genuchten and Mualem hypotheses (Mualem 1976), are applicable to nonwoven geotextiles. Thus, both of these constitutive equations were employed to approximate WRC and permeability functions for both the soil and the nonwoven geotextile.

$$S_e = \frac{S - S_{res}}{S_{sat} - S_{res}} = \left[1 + (g_a |h_p|)^{g_n} \right]^{g_c} \quad (1)$$

$$k_r(S_e) = S_e^{0.5} \left[1 - (1 - S_e^{-1/g_c})^{-g_c} \right]^2 \quad (2)$$

where S_e is the effective degree of saturation, S is the degree of saturation, S_{res} is the residual saturation at a very high value of suction, S_{sat} is the saturation of saturated soil, h_p is the matric suction head, k_r is the relative permeability coefficient. g_a [m^{-1}], g_c and g_n are fitting parameters, and according to the Mualem hypothesis (Mualem 1976), g_c is assigned a value of $1/g_n - 1$.

3. PHYSICAL EXPERIMENTS

Figure 1 shows large-scale physical experiments of MSE wall model conducted to simulate a practical scenario, in which MSE wall undergoes a leveling of groundwater table. The bottom, left and right sides of the physical model were established as impervious boundaries. Four standpipe piezometers, 10 surface settlement plates and 10 TDR probes were installed to measure water level, settlement and volumetric water contents during seepage flow, respectively. During the test, groundwater flows were controlled by observing the change in water level in the upstream and downstream water tanks. The water level in the downstream water tank was kept constant at the toe of the wall (+0.0 m) using a control weir. The water level in the upstream tank was increased stepwise from heights of +0.0 m, +0.4 m, +0.7 m, and +1.0 m, respectively. The upstream water level was continuously increased after a steady state was gained, in which there was no change in the water content values, read from the TDR probes, for a period equal to or greater than 24 h. This scenario was established to simulate the most severe situation, at which the groundwater level behind an MSE wall was very high, similar to the situation that may occur in mountainous areas during heavy rainfalls. The shallow soil layer was assumed to be underlain by a bedrock layer, such that inundation might be occurred during a heavy rainstorm (Figure 1b).

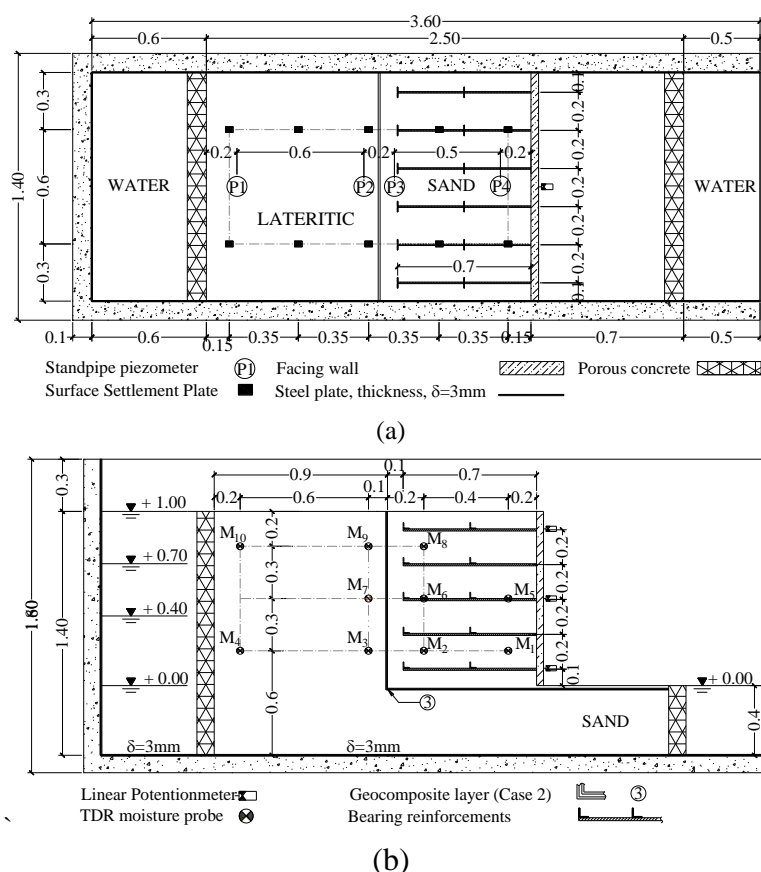


Figure 1 Sketch of the physical test and its instrumentation: (a) plan view and (b) side view of the model

4. NUMERICAL EXPERIMENTS

A series of numerical experiments was subsequently conducted to investigate the effect of the relevant material properties on the flow response through the MSE wall, with a geocomposite drain installed, using the finite element code Plaxis 2D. The discretised plane strain finite element mesh is shown in Figures 2a and 2b for the MSE wall without and with geocomposite drain installation, respectively. A triangular mesh was used in the numerical model. Although a rectangular mesh is commonly adopted in water flow models, it has been reported that the calculated results do not depend on the type of mesh because the interpolation function in flow problems is linear (Potts and Zdravković 2001).

In Plaxis, there are two well-known types of triangular elements: 6-node triangles and 15-node triangles. In this study, 15-node triangles were assigned to the models. The use of 15-node triangles yields more accurate calculation results than that of 6-node triangles. A fine mesh with an average element size of 0.033 m was assigned. A finer mesh was also assigned to the geotextile and the geonet. The initial conditions of the model were defined based on the controlled density and water content during the placement of compacted soil in the physical box. Dirichlet boundary conditions with prescribed pressures were imposed on the left, right, and upper boundaries of the model. The bottom boundary of the model was defined as impermeable. In Plaxis, the time steps were assigned automatically for steady-state calculation. At each time step, a modified Newton-Raphson model was used to solve the relevant equations iteratively. In each iteration, increments of the groundwater head were calculated from the imbalance in the nodal discharges and added to the active head. This process was continued until the norm of the unbalance vector, i.e., the error in the nodal discharges, was smaller than that of the tolerated error of 0.01 (or 1%).

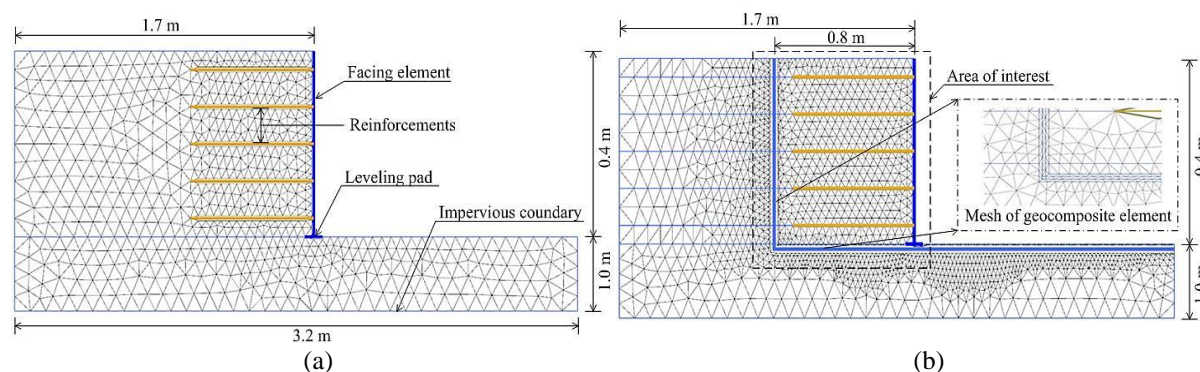


Figure 2 Mesh discretisation of the models (a) without and (b) with geocomposite installation

5. MATERIALS

The soils used in this investigation were a sandy soil and a lateritic soil. The sandy soil was classified as poorly graded sand (SP), according to the Unified Soil Classification System (USCS), with its specific gravity of 2.74. The compaction characteristics under standard Proctor energy were optimum water content (OWC) of 5.7% and maximum dry unit weight $\gamma_{d,max}$ of 16.7 kN/m³. The saturated hydraulic conductivity of the soil was k_{sat} = 17 m/day. For the lateritic soil, it was classified as SM-SC, with the specific gravity of 2.75. The compaction characteristics of the lateritic soil were 5.7% of optimum water content and 16.7 kN/m³ of maximum dry unit weight. The saturated hydraulic conductivity of the soil was k_{sat} = 0.3456 m/day.

Determinations of the WRC of the soil were conducted along the drying and wetting paths. The drying phase WRC was obtained using a pressure plate apparatus and the wetting phase WRC was obtained from the double-walled triaxial cell. The relationships between volumetric water content and matric suction of the sandy soil, lateritic soil and geotextile are presented in Figure 3.

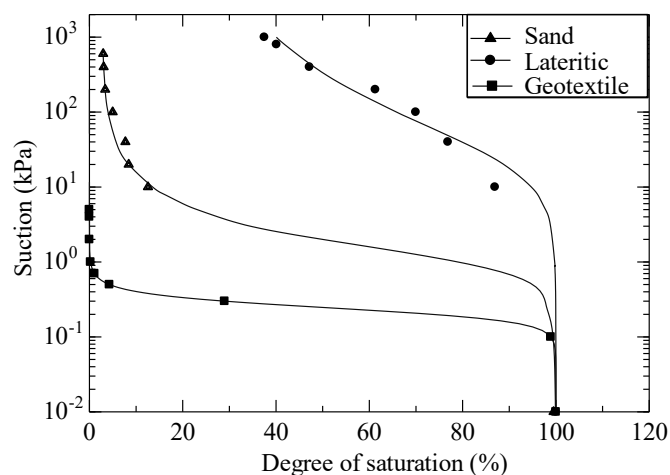


Figure 3 WRC curves of the materials used in this study

6. MODEL CALIBRATION

Figure 4 presents the measured (with symbols) and calculated (with lines) water levels and volumetric water contents for the various upstream water levels for tests without (Figure 4a) and with (Figure 4b) geocomposite installation. The water levels and the volumetric water contents presented in Figure 5 were those measured at 18 days, 21 days, and 23 days, which represent the end times of upstream water levels of +0.4 m, +0.7 m, and +1.0 m, respectively. At any upstream water level height, the water level decreases through the wall face. The measured water level data for case I (no geocomposite) were compared to those for case II (with geocomposite). The comparisons show that the highly permeable geocomposite can effectively prevent water flow to the reinforced zone (or protected zone), as it collects the water in the unreinforced zone and drains it out at the wall face.

Figures 4 also compares the measured and calculated phreatic surface, distribution of volumetric water content at various heights of the upstream water level. The numerical model yields a variation in the phreatic surface similar to that measured in the tests. Fair agreement between the measurements and the corresponding calculations for the two cases was found.

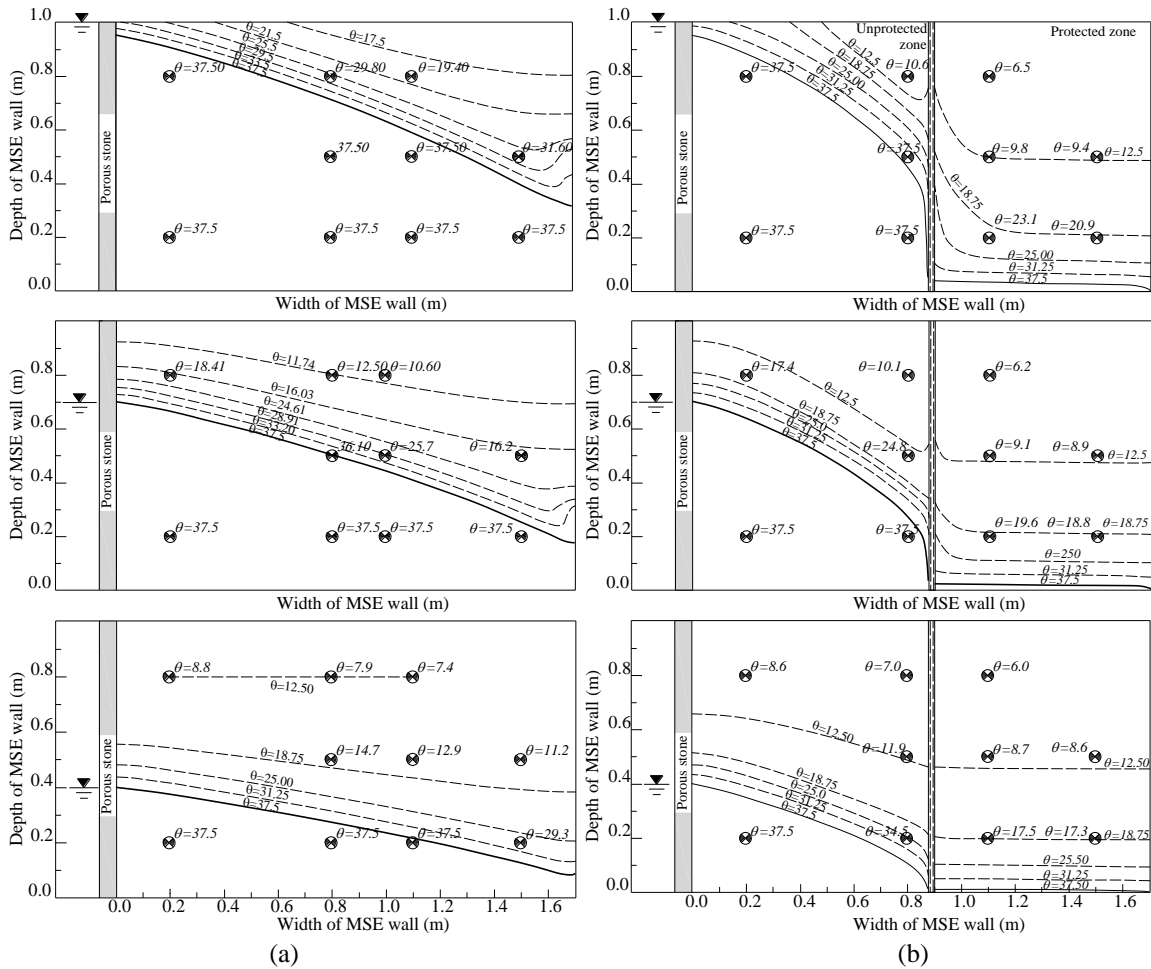


Figure 4 Measured and calculated phreatic surfaces and water contents for MSE wall
(a) case I (without geocomposite drain installed) and
(b) case II (with geocomposite drain installed)

7. PARAMETRIC STUDY

The hydraulic responses represent the effective saturation and phreatic surface, determined from numerical experiments are presented and discussed within this section. The effect of the hydrological properties of the soil and the geotextile on the hydraulic response was evaluated using (1) van Genuchten parameters (g_a and g_n) and (2) the corresponding saturated permeability. For the hydrological properties of the geonet, only the saturated hydraulic conductivity of the geonet was evaluated.

In general, it was found that the phreatic surface outside the protected zone was not notably changed within the range of considered parameters indicated in Table 1. The phreatic surface in the protected zone and the distribution of effective saturation were affected by some of the considered parameters, as discussed in this section.

Table 1 VG and VGM model parameters and saturated hydraulic conductivity of the materials used in this study

| Parameter | Lateritic soil (unprotected zone) | Sandy soil (protected zone) | Geotextile | Geonet |
|--------------------|-----------------------------------|-----------------------------|------------|-------------|
| K_{lat} [m/day] | 0.00346-300 | 17 | 17-4000 | 2000-100000 |
| K_{long} [m/day] | 0.00346-300 | 17 | 50-2000 | 2000-100000 |
| g_a [m^{-1}] | 0.5-5 | 20 | 2.5 | 600 |
| g_n [-] | 1.1-1.5 | 1.5 | 20 | 40 |
| S_{res} [-] | 0.2 | 0.03 | 0.03 | 0 |
| S_{sat} [-] | 1.0 | 1.0 | 0.8 | 1 |

7.1. EFFECTS OF THE VAN GENUCHTEN PARAMETERS OF FILL MATERIAL

7.1.1. THE VAN GENUCHTEN PARAMETER g_a

Figures 5a and 5b present the effective saturation profiles along sections a-a and b-b, respectively, for various magnitudes of g_a . The alignment of these sections (a-a) and (b-b) are vertical and located at 0.05 m to the left and right from the geocomposite drainage. At a certain depth above the phreatic surface, the soil with a low g_a value exhibits high saturation inside the unprotected zone. The degree of saturation was found to decrease when the magnitude of g_a decreases. In short, the wet zone spreads more widely for the low g_a soil than for the high g_a soil. However, Figure 5b clearly shows that the variation of g_a parameter of outer soil slightly affect the effective saturation profiles in the reinforced zone.

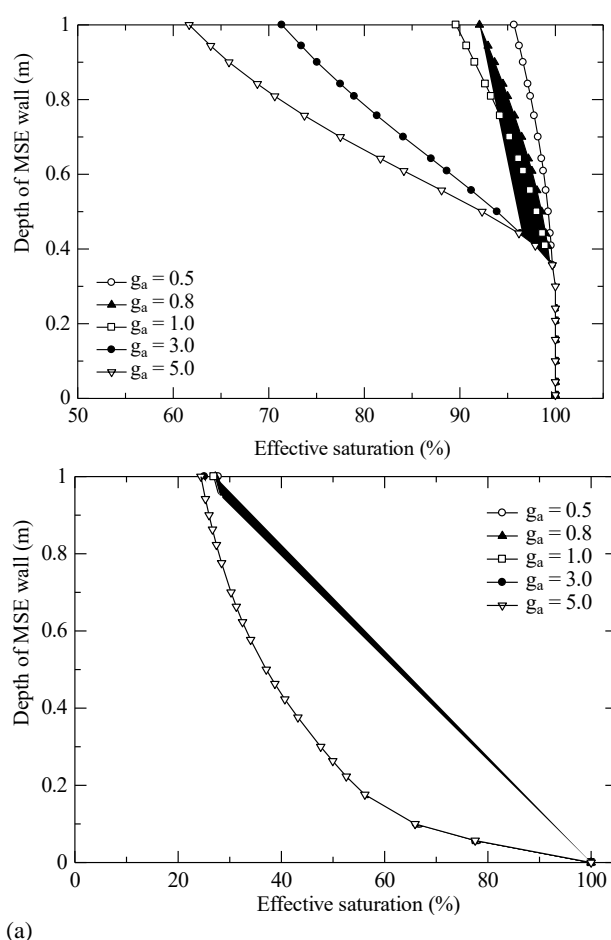


Figure 5 : Effective saturation profile along vertical sections located (a) 5 cm left and (b) 5 cm right of the geocomposite for various magnitudes of g_a of outer soil

7.1.2. THE VAN GENUCHTEN PARAMETER g_n

Figure 6 presents phreatic surface and effective saturation contour lines in the MSE wall model calculated at various magnitudes of g_n of the outer soil. The results show that effective saturation (outside the protected zone) clearly depends on the magnitude of g_n the wider distribution of effective saturation was found with a lower g_n . However, figure 6 indicates that the variation of g_n of outer soil slightly affect the effective saturation inside the reinforced zone.

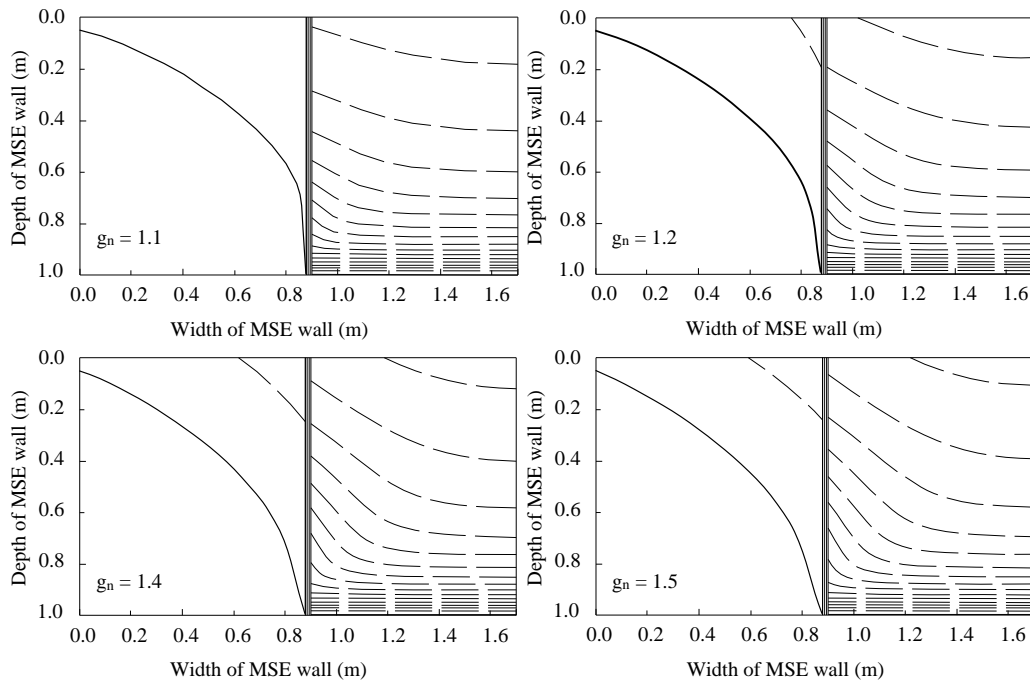


Figure 6 Phreatic surface (solid line) and effective saturation contour lines (dash line) in the MSE model for various magnitudes of g_n of soil

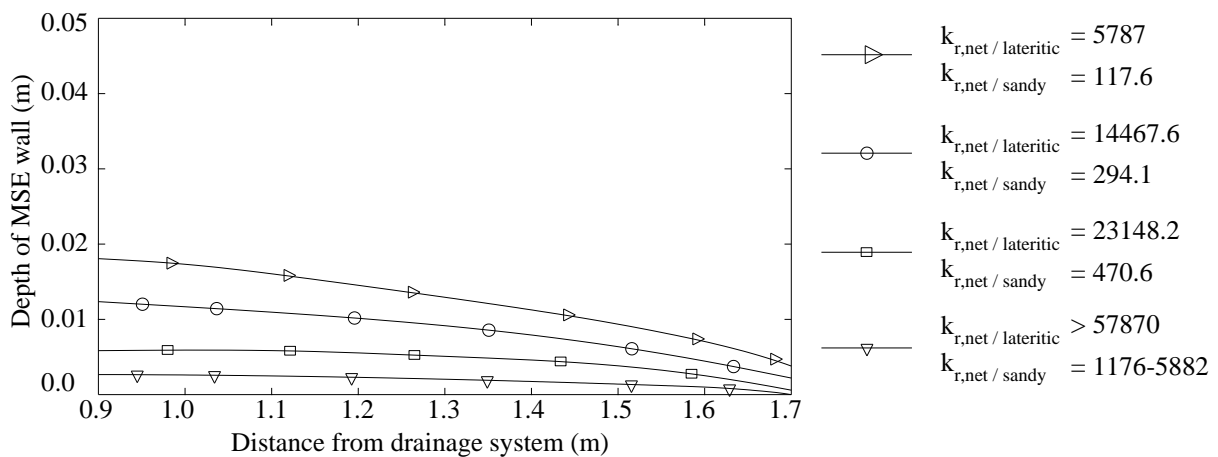


Figure 7 Variation in phreatic surface in the protected zone for various ratios between the hydraulic conductivity of the geonet and that of soil

7.2. EFFECT OF HYDRAULIC CONDUCTIVITY RATIO

The level of the phreatic surface inside the protected zone is vital to the stability of the MSE wall. The lower phreatic surface level results in a lower water content inside the protected zone, and hence a higher stability for the wall might be gained. Chinkulkijniwat et al. (2016) presented the effect of the ratio between the hydraulic conductivity of the geonet and that of sandy soil ($K_{r,net/sandy}$) on the phreatic surface in the protected zone. A large $K_{r,net}$ value was found at the lower phreatic surface level in the protected zone. Further reduction of the phreatic surface level was not observed when the magnitude of $K_{r,net}$ was greater than 1765. From these results, they concluded that the phreatic surface level in the protected zone was mainly governed by the magnitude of $K_{r,net}$. Figure 7 shows the variation of phreatic surface level at various magnitudes of the ratio between the hydraulic conductivity of the geonet and that of lateritic soil ($K_{r,net/lateritic}$) ranged from 5787 to 289351. It clearly shows that the $K_{r,net/lateritic}$ in protected zone does not affect phreatic surface level inside the reinforced zone within the range of the studied $K_{r,net/lateritic}$. Therefore, the result in this study is confirmed by the finding from Chinkulkijniwat et al. (2016).

8. CONCLUSIONS

The drainage ability of geocomposites which consists of a core material with a large flow channel (geonet) sandwiched by two nonwoven geotextile layers, was investigated through large-scale MSE wall model tests. The experimental results indicate that the geocomposite studied effectively prevents the flow of water into the reinforced zone by collecting water in the unreinforced zone and draining it in front of the wall face. Comparisons between the deformations of the MSE wall models with and without geocomposite installation indicate that the MSE wall with a geocomposite is far superior to that without a geocomposite. Numerical models were established to conduct parametric studies. The following conclusions can be drawn as a result of this research.

- (1) The WRC parameters of the soil do not reflect the distribution of effective saturation in the soil both inside reinforced zone.
- (2) The ratio between the hydraulic conductivity of the geonet and that of lateritic soil the ($K_{r,net/lateritic}$) in protected zone does not affect phreatic surface level inside the reinforced zone.

9. REFERENCES

1. Koerner, R.M., Soong, T-Y. (2000), "Stability assessment of ten large landfill failures." *Geotechnical*. Vol.103: 1-38.
2. Shibuya, S., Saito, M., Torii, N., and Hara, K. (2009), "*Mitigating embankment failure due to heavy rainfall using L-shaped geosynthetic drain*", Proceedings of the International Symposium on Prediction and Simulation Methods for Geohazard Mitigation, Kyoto, Japan, (229-306).
3. Koerner, R.M., (2005). *Designing with Geosynthetics*. 5th Edition. Englewood Cliffs, New Jersey : Prentice Hall Publ. Co.
4. Yoo, C., & Jung, H. Y. (2006), "*Case history of geosynthetic reinforced segmental retaining wall failure*" *Journal of Geotechnical and Geoenvironmental Engineering*. Vol.132 No.12 : 1538-1548.
5. Stormont, J. C., Morris, C. E. (2000), "*Characterization of unsaturated nonwoven geotextiles*" *Advances in unsaturated geotechnics*, ASCE. (153-164)
6. Lafleur, J., Lebeau, M., Faure, Y. Savard, Y., Kehila, Y. (2000), "*Influence of matric suction on the drainage performance of polyester geotextiles*" The 53rd annual conference of Canadian Geotechnical Society, Motreal, Canada. Vol.2 : 1115-1122.
7. Ho, A.F. (2000), "*Experimental and numerical investigation of infiltration ponding in one-dimensional sand-geotextile columns*". M.Sc. Thesis, Queen's University, Kingston, Ont., Canada.
8. Knight, M.A., Kotha, S.M. (2001), "*Measurement of geotextile-water characteristic curves using a controlled outflow capillary pressure cell*" *Geosynthetics International*. Vol.8 No.3 : 271-282.
9. Iryo, T., Rowe, R.K. (2003), "*On the hydraulic behavior of unsaturated nonwoven geotextiles*" *Geotextiles and Geomembranes*. Vol.21 : 381-404.
10. Iryo, T., Rowe, R.K. (2004), "*Numerical study of infiltration into a soil-geotextile column*" *Geosynthetics International*. Vol.11 No.5 : 377-389.
11. Bouazza, A., Freund, M., Nahlawi, H. (2006b), "*Water retention of nonwoven polyester geotextiles*" *Polymer Testing*. Vol.25 No.8 : 1038-1043.
12. Nahlawi, H., Bouazza, A., & Kodikara J. (2007), "*Characterisation of geotextiles water retention using a modified capillary pressure cell*" *Geotextiles and Geomembranes*. Vol.25 No.3 : 186-193.
13. Van Genuchten, M. Th. (1980), "*A closed-form equation for predicting the hydraulic conductivity of unsaturated soil*" *Soil Science Society of America Journal*. Vol.44 No.5 : 892-898.
14. Mualem, Y. (1976), "*A new model for predicting the hydraulic conductivity of unsaturated porous media*" *Water Resources Research*. Vol.12 No.3 : 513-522.
15. Chinkulkijniwat, A., Horpibulsuk, S., Bui Van, D., Udomchai, A., Goodary, R., & Arulrajah, A. (2016), "*Influential factors affecting drainage design considerations for mechanical stabilised earth walls using geocomposites*". *Geosynthetics International*. (1-18).